Understanding the Accelerating Effect of ϵ-Caprolactam on the Formation of Urethane Linkages

Monica Bertoldo,† Chiara Cappelli,† Stefano Catanorchi,‡ Vincenzo Liuzzo,‡ and Simona Bronco*,†

PolyLab-INFM, c/o Dipartimento di Chimica e Chimica Industriale, Università di Pisa, via Risorgimento 35, I-56126 Pisa, Italy, and Dipartimento di Chimica e Chimica Industriale, Università di Pisa, via Risorgimento 35, I-56126 Pisa, Italy

Received September 15, 2004; Revised Manuscript Received November 19, 2004

ABSTRACT: The accelerating role of ϵ-caprolactam on the formation of urethane linkages is studied in the case of the reaction between toluene 2,4-diisocyanate and n-propanol in carbon tetrachloride at room temperature. FT-IR spectroscopy is exploited to follow the consumption of the isocyanate groups. The comparison between the rate of the reactions carried out in the presence and absence of a catalytic amount of ϵ-caprolactam shows its accelerating effect. The acylurea-like derivative 1-methyl-2,4-[(2-oxoazepane-1-carbonyl)amino]benzene has been prepared and identified as the real catalytic species formed in situ as a result of the reaction between toluene 2,4-diisocyanate and ϵ-caprolactam. A kinetic model is proposed to analyze the experimental data, and B3LYP/6-31+G* calculations are exploited to investigate the structure of 1-methyl-2,4-[(2-oxoazepane-1-carbonyl)amino]benzene and clarify the structural features leading the catalytic activity.

1. Introduction

In this paper, the accelerating effect due to the presence of catalytic amounts of ϵ-caprolactam in the polyurethane formation and cross-linking is studied. To model the reaction between isocyanate and hydroxylic groups, which is industrially exploited to obtain polyurethane linkages,[1,2] the reaction between toluene 2,4-diisocyanate and n-propanol in carbon tetrachloride solution is here chosen.

The industrial use of ϵ-caprolactam as a curing agent for the polyurethane coating is reported in a few patents:[3] however, to the best of our knowledge, no detailed studies aimed at rationalizing its accelerating effect in the polyurethane formation and cross-linking are present in the literature. On the other hand, ϵ-caprolactam is a well-known blocking agent for polyurethanes,[4] and it is widely used to produce one-package coatings. In this field, isocyanates are reacted with a compound containing active hydrogens, and after heating in the presence of a nucleophilic species, the isocyanate is reobtained. The deblocking temperature depends on both isocyanate and blocking agent, in the case of ϵ-caprolactam ranging between 130 and 160 °C.

Generally speaking, the urethanes formation reaction can be seen as an addition of a nucleophilic species (the alcohol) to an electrophilic center (the isocyanate), and it can be catalyzed by both Lewis acids and bases. In particular, synergistic effects on increasing the rate of formation of urethanes has been observed when both an acid and a base are used at the same time.[5] Amides, carbamates, and ureas, as all nucleophilic compounds, have been experimentally proven to accelerate the formation of polyurethanes, even if their catalytic efficiency is less than that of amines.[6] Among the carboxylated compounds mentioned above, the accelerating effect increases in the order carbamates < amides < ureas. In addition, acidic amides are reported to act as bifunctional catalysts, thus promoting the alcoholysis through a cyclic proton transfer.[5]

Many papers reporting studies on the mechanism of the urethanes formation reaction from isocyanates and alcohols, in both the presence and absence of catalytic species, are present in the literature.[2,5−7] In the pioneering works performed before the 1960s (see ref 7 and references therein), a second-order kinetics was assumed, whereas in following studies the role of alcohol clusters was evidenced and a higher reaction order with respect to the alcohol was assumed. Studies on the influence of alcohol clusters on the mechanism of urethanes formation have been carried out in various experimental conditions (such as different alcohol/isocyanate pairs, different absolute values of the reactant concentrations, different solvents, presence or absence of catalysts, different kinds of catalysts, etc.) and have shown the influence of the change in the various parameters on the reaction mechanism. For example, it has been reported that the mechanism associated with the kinetics model requires one or more alcohol molecules participating in the transition state, as is illustrated in Schemes 1 and 2.[5−8]

Two different mechanisms, sketched in Schemes 3 and 4, have been proposed for the reaction catalyzed by a tertiary amine, differing in the center attacked by the amine in the first step of the process. Both the proposed mechanisms involve the same four-centered intermediate in the second step.[9,10] When different amines are used as catalysts, the reaction rate was experimentally found to increase as the basicity of the amine increases and its steric hindrance decreases.[11]

In most of the papers the mechanism of urethane formation has been studied on model reactions involving two monofunctional molecules. The influence of solvent polarity and hydrogen-bonding capability have been analyzed, showing that solvent effects are a balance between the ability of stabilizing a four-center activation

† PolyLab-INFM.
‡ Dipartimento di Chimica e Chimica Industriale.
* Corresponding author: Ph +39 050 2219447; Fax +39 050 2219320; e-mail simona@dcci.unipi.it.

10.1021/ma0480998 CCC: $30.25
Published on Web 01/27/2005

Scheme 1

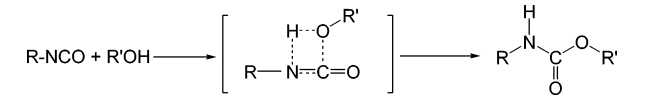

Scheme 2

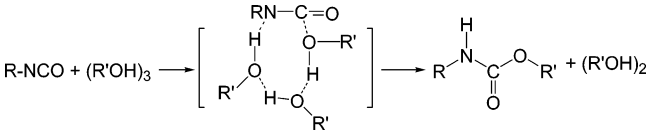

Scheme 3

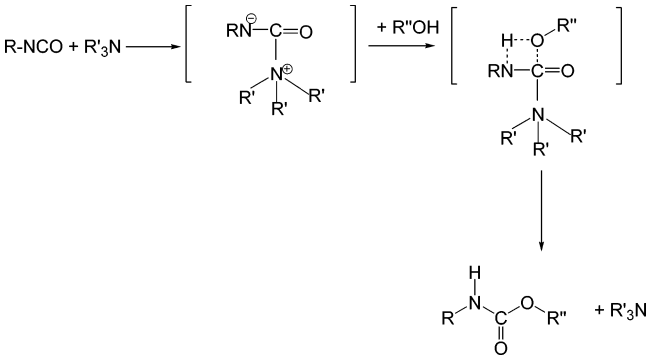

Scheme 4

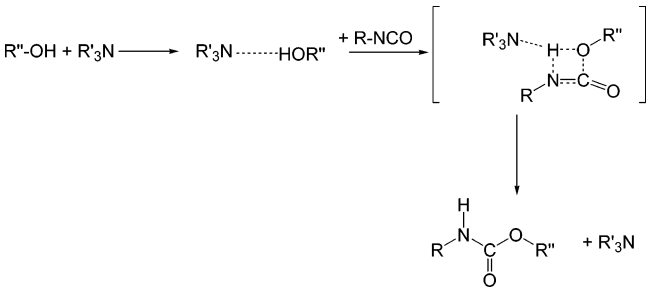

complex and the strength of the solvent−alcohol interaction, which decreases the alcohol reactivity.[7,12] Several studies have also analyzed the effect of the mutual influence of functional groups in polyfunctional monomers by studying both the reaction between diisocyanates and alcohols and the reaction between (mono)-isocyanates and glycols.

In polymerization reactions, additional complications arise from the different reactivity of the dimers, differences in reactivity between the functional terminal groups of growing chains at different molecular weights, and the continuous modification of the reaction environment due to the polymer chain growth.

The different experimental approaches which can be used to study the (poly)urethane formation mechanism have already been summarized elsewhere, and advantages and disadvantages have been pointed out.[7] In this work a stoichiometric alcohol/isocyanate ratio is used, which is kept constant at the initial concentration, and FT-IR is used to both follow the reaction and, together with mass spectroscopy, analyze the products.

The paper is organized as follows: after the presentation of the experimental methodologies used to carry out the study, a discussion of the reaction which is here exploited to model the formation of polyurethane linkages is reported. Then, a kinetic analysis of the reaction is given, and the nature of the active catalytic species is clarified. To identify the structure and chemical features of the catalytic species, quantum mechanical calculation are reported. A short summary and some drawn conclusions end the presentation.

2. Experimental Part

2.1. Materials. CCl_4 (Aldrich) and $CHCl_3$ (Aldrich) were dried on molecular sieves and stored under a nitrogen atmosphere; toluene 2,4-diisocyanate (TDI) (Aldrich) was distilled under a 10 mmHg nitrogen atmosphere at 119−120 °C; ϵ-caprolactam (99%, Aldrich) and n-propanol (n-PrOH) (Aldrich) were used as received.

2.2. Synthesis of 1-Methyl-2,4-[(2-oxoazepane-1-carbonyl)amino]benzene (AC). TDI (2 g, 0.0114 mol) and ϵ-caprolactam (2.86 g, 0.025 mol) were refluxed for 8 h, under a N_2 atmosphere, in 10 mL of CCl_4. The precipitate was filtered, washed with ethanol and Et_2O, air-dried, and recrystallized from $CHCl_3/Et_2O$ to yield 4.3 g (94%) of a white powder; mp = 150 °C. FT-IR (KBr, Nujol, cm^{-1}): 1654 (C=O), 1707 (C=O), 3326 (N−H). ^1H NMR ($CDCl_3$, 200 MHz): δ 11.44 (s, 2H, N−H), 8.23 (d, 1H, Ar−H), 7.26 (d, 1H, Ar−H) 7.10 (d, 1H, Ar−H), 4.07 (t, 4H), 2.78 (t, 4H), 2.28 (s, 3H), 1.78 (m, 6H). ^{13}C NMR ($CDCl_3$): δ 179.8, 151.9, 136.6, 136.2, 130.2, 123.6, 116.1, 113.6, 43.7, 39.8, 29, 28.2, 23.5, 17.6, 17.3. ESI-MS (*m/z*): 401 ($[M-H]^+$), 418 ($[M-Na]^+$), 423 ($[M-NH_4]^+$). GC-MS (min; *m/z*): 16.43, 113 (ϵ-caprolactam), 17.82; 174 (TDI).

2.3. Methodologies. ^1H and ^{13}C NMR spectra were recorded at room temperature with a Varian-Gemini 200 MHz spectrometer from solutions in $CDCl_3$ and were referred to TMS as external standard. IR spectroscopy analyses were performed with a Paragon 500 (Perkin-Elmer) spectrophotometer. The melting point was measured with a Reichert Thermovar analyzer.

ESI mass spectra were recorded on a PE Sciex API III plus triple quadrupole mass spectrometer equipped with an atmospheric pressure ionization source and an articulated ionspray interface. The sample was dissolved in chloroform (1 mg/mL) and diluted 1:1000 with acetonitrile. Experimental conditions included IS voltage (5.5 kV) and OR voltage (90 V).

Solutions of the synthesis products in chloroform were analyzed by gas chromatography (HP, GCD series II) coupled with mass spectrometry (MS). The injections were carried out by using the splitless mode and keeping the injector temperature at 280 °C. Separation was performed using a 30 m 0.25 mm i.d. capillary column with a film thickness of 0.25 μm. Helium fluxing constant at 1 mL/s served as the carrier. The GC oven temperature was first held at 35 °C for 6 min, increased to 200 °C at a rate of 10 °C/min, held there for 1 min, and then increased at 15 °C/min up to the final temperature of 280 °C, which was kept fixed for 5 min. Mass spectra acquisition, processing, and instrument control were performed using HP Chemstation software. Electron impact (EI) mass spectra were obtained at 2300−2400 eV electron energy and monitored from 45 to 450 *m/z*.

Kinetics studies were carried out at room temperature by following the decrease of the height of the IR stretching band of isocyanate at 2265 cm^{-1}. The spectra were recorded with a FT-IR Perkin-Elmer 1330 spectrophotometer interfaced with an Infrared Data Base model 3600. CaF_2 or KBr cells for liquids (having 5.19×10^{-3} cm and 9.82×10^{-3} cm thickness, respectively) were filled with solutions obtained by mixing suitable amounts of the following solutions: TDI (0.03325 M in CCl_4), n-PrOH (0.0663 M in CCl_4), ϵ-caprolactam (0.072 M in CCl_4), and AC (0.03443 M in $CHCl_3$).

Computational Details. All the quantum mechanical calculations were carried out by using density functional theory (DFT)[13] as implemented in the Gaussian package.[14] The gradient-corrected hybrid functional B3LYP[15] was used in all the calculations. The 6-31G* basis set[16] was used in the geometry optimizations: the wave function analyses were done with the 6-31+G* basis set on the B3LYP/6-31G* geometries. The NBO analysis[17] was performed by using the NBO module in Gaussian03.[14] The Bader's atoms in molecules analysis[18] was performed by exploiting the AIM2000 program.[19] The calculations in solution were done by exploiting the polarizable

continuum model[20] as implemented in Gaussian03. In the calculations in solutions a molecular-shaped cavity was used, which was built by interlocking spheres having the following radii: 2.28 Å for aromatic C−H groups, 2.4 Å for CH_3 and CH_2 groups, 2.04 Å for N and sp^2 and sp C atoms, 1.824 Å for O atoms, and 1.44 Å for acidic H atoms. The following values for the static dielectric constant of the solvents were used: 2.228 for CCl_4, 4.9 for $CHCl_3$, and 20.1 for n-PrOH.

3. Results and Discussion

3.1. Selection of the Model. The study of the activation mechanism of ϵ-caprolactam on the chain extension and cross-linking of polyurethane coatings is complex because of the many variables affecting the reactivity of the system. Moreover, most of the effects, such as the influence of the environment and the reactivity of the groups, which may depend on the dimension of the growing chains, change as the reaction proceeds. It was reported that complex models have to be used to describe the kinetics of polyurethane formation.[1] For this reason, to simplify the study and to make it possible to understand the details of the mechanism and the kinetic features, the reaction between TDI and n-PrOH (A) was chosen as model of the addition reaction involved in the formation of polyurethanes.

TDI was selected because it is widely used as starting material for the production of polyurethanes.

A monohydroxyl alcohol was used instead of a glycol in order to focus the study on urethane function in absence of the physical modifications of the reaction environment typically associated with the formation and growth of polymeric chains. Moreover, the reactivity of both −NCO and −OH remains constant during the reaction time, and only the difference in reactivity between the two isocyanic groups is to be taken into account.

The choice of CCl_4 as reaction solvent is first of all due to the fact that all reactants are soluble in it, and in addition, it does not cover the IR absorption band of isocyanate used to follow the formation of urethane linkages. Last, CCl_4 should not be involved in hydrogen bonds with the reactants, which have been reported to influence the reaction mechanism and kinetics.[7,8e]

3.2. The Reaction Model and Its Kinetics. The behavior in time of the IR spectrum of the solution absorbance by mixing equal amounts of the solutions of TDI and n-PrOH is reported in Figure 1: as expected, the decrease of the stretching band of the isocyanate group (2265−2274 cm^{-1}) is observed (Figure 1A). Notice that the maximum peak height was monitored instead of the area because the absorption at 2270 cm^{-1}, due to the CO_2 present in the measure chamber, is partially superimposed to the isocyanate absorption and could not be completely eliminated by the instrument software. Further inspection of Figure 1A reveals the appearance and the increase in the bands at 1741 ($\nu^{C=O}$ carbamate), 1525 ($\nu^{C=O}$ of the associate carbamate), 1416 (ν^{C-N}), and 3445 cm^{-1} (ν^{N-H} carbamate), all indicating the formation of urethane-type linkages. In addition, the increase in the band at 1597 cm^{-1} and the corresponding decrease in the band at 1618 cm^{-1} (which can be assigned to the stretching of the carbon−carbon bonds of the aromatic ring of products and reactant, respectively) were observed. Moving to the analysis of the behavior of Figure 1B, the IR spectra in the range between 3800 and 3300 cm^{-1} as a function of the time show the increase in the intensity of the N−H stretching band at 3445 cm^{-1}, whereas the O−H stretching band

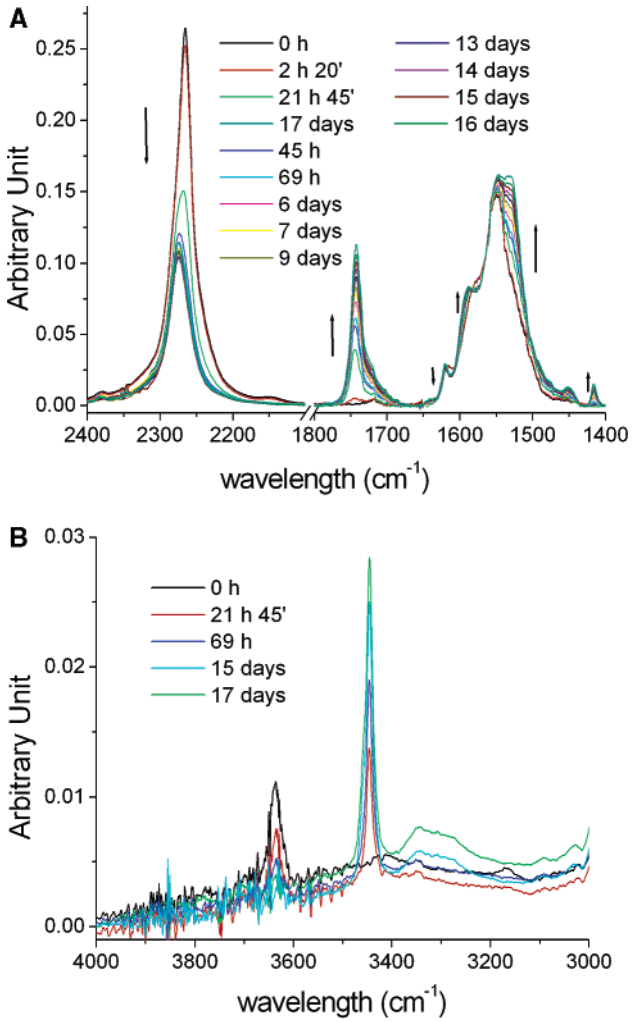

Figure 1. IR spectra of the TDI/n-PrOH mixture (0.0166/0.0332 by mole in CCl_4) in a CaF_2 IR cell for liquid at different reaction times: (A) in the range between 1400 and 2400 cm^{-1}; (B) in the range between 3000 and 4000 cm^{-1}.

typically associated with the formation of alcohol clusters[7] decreases.

The addition of 5 mol % of ϵ-caprolactam to the TDI/n-PrOH mixture accelerates the decreasing rate in the intensity of the IR stretching band of the isocyanate, as is shown in Figure 2. In particular, in this case the unreacted isocyanate is not detectable anymore at the time corresponding to the reaching of about 30% of the initial value in the reference reaction (i.e., without catalyst).

To investigate in more detail the possible reactions between TDI and ϵ-caprolactam, their CCl_4 solution were mixed together with a 1:2 ratio. The decrease in the stretching band of the isocyanate and the appearance and the following increase in intensity of two bands at 1641 and 1591 cm^{-1} indicate the consumption of TDI and the formation of an acylurea linkage. These findings suggest that, as a result of the reaction between TDI and ϵ-caprolactam, acylureic groups are formed, and in particular, the formation of a diadduct-like species (AC) is here suggested (see Scheme 5). The possibility of formation of AC is in agreement with the well-known reaction between ϵ-caprolactam and isocyanate groups, leading to the formation of "blocked" isocyanic groups which can easily be recovered by heating.[4]

The kinetics of the relative decrease in the isocyanate stretching band in the reaction of TDI with n-PrOH and

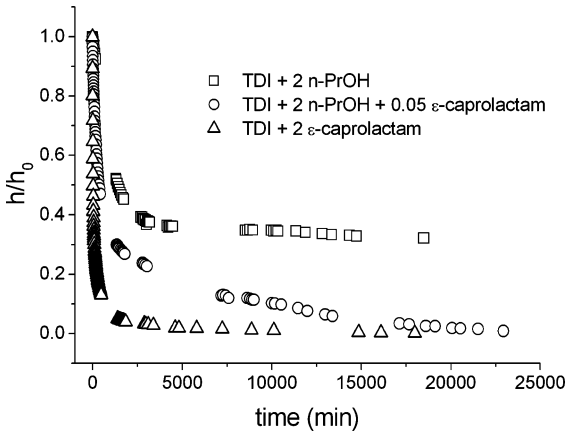

Figure 2. Comparison among the experimental decrease in time of the relative maximum absorbance of the IR stretching band of isocyanate in the range 2200−2300 cm^{-1} for the reactions listed in the legend which were all carried out with a 0.0166 M starting concentration of TDI and by using CCl_4 as solvent.

Scheme 5

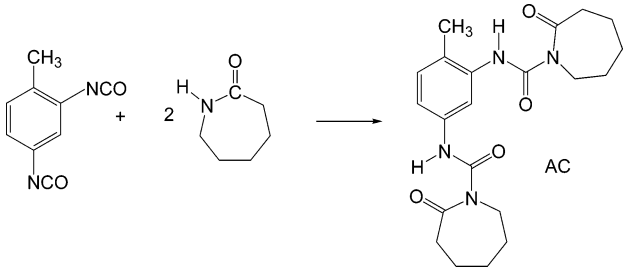

ϵ-caprolactam are compared in Figure 2 with the other cases here studied. It is evident that the reaction between TDI and ϵ-caprolactam is much faster than the others.

The analysis by IR, NMR, and GC-MS of the TDI/ϵ-caprolactam/n-PrOH (4.3/8.6/8.6 mmol) mixture stirred for 8 days at room temperature in 9 mL of CCl_4 reveals the presence of several compounds, among them the products resulting from the mono- and diaddition of n-PrOH to TDI and addition products of ϵ-caprolactam to TDI. Moreover, unreacted n-PrOH and ϵ-caprolactam (in traces) are also present.

From the resulted presented so far, the following points can be issued:

• The reaction between TDI and n-PrOH gets faster if a catalytic amount of ϵ-caprolactam is added to the mixture.

• Both ϵ-caprolactam and n-PrOH can react with TDI at room temperature; however, the reaction between TDI and ϵ-caprolactam is faster than the one between TDI and n-PrOH. The formation of AC in the TDI/n-PrOH/ϵ-caprolactam (1/2/0.05) mixture can occur in the initial stages.

To investigate a possible role of AC in accelerating the reaction between TDI and n-PrOH, it was synthesized and characterized. Then, the decrease in time of the IR stretching band of isocyanate of a TDI/n-PrOH/AC (1/2/0.025 mol) mixture was monitored. The behavior of IR spectra of the mixture at different observation times, which is reported in Figure 3, is similar to that observed for the uncatalyzed reaction (compare Figure 1). In addition, the appearance and increase of a band at 1645 cm^{-1} are also evidenced. This band can be addressed to the formation of small amounts of urea

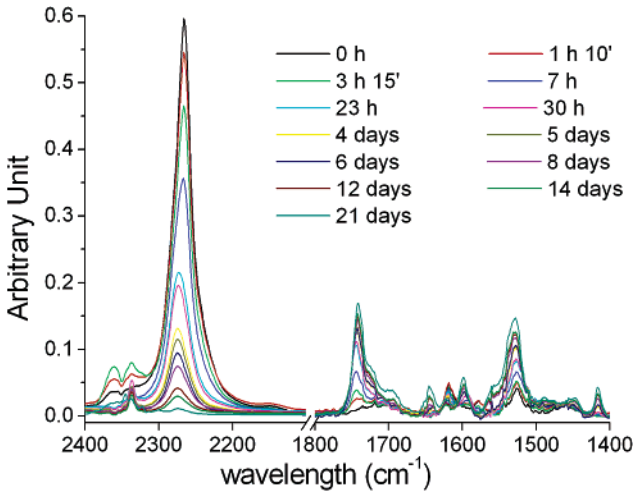

Figure 3. IR spectra in the range between 1400 and 2400 cm^{-1} of the TDI/n-PrOH/ϵ-caprolactam mixture (0.0166/0.0332/0.00018 M in CCl_4) in a KBr IR cell for liquid at different reaction times. Solvent contribution has been subtracted.

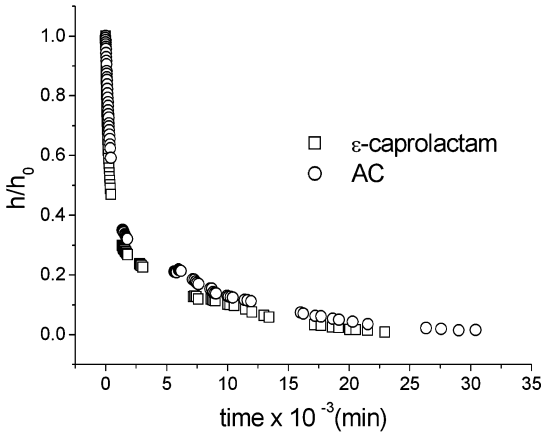

Figure 4. Comparison between the experimental decrease in time of the relative maximum absorbance of the IR stretching band of isocyanate in the range 2200−2300 cm^{-1} for the reaction between TDI and n-ProH (0.0166/0.0332 M in CCl_4) carried out in the presence of a catalytic amount (1 mol % of catalyst with respect to TDI) of ϵ-caprolactam or AC.

linkages deriving from the reaction between aromatic amines and isocyanate. The formation of the aminic derivatives is confirmed by the increase in the intensity of the peak at 2237 cm^{-1} due to CO_2 in solution: this peak, which is observed at a longer reaction time, is typically associated with the decomposition of TDI as a result of the reaction with water.[1]

In Figure 4, the kinetics of the reactions between TDI and n-PrOH both in the presence of AC and of an equivalent amount of ϵ-caprolactam are reported. As it is clearly shown, the two kinetics are comparable. Thus, from the data shown so far it seems possible to infer that the actual catalyst in the reaction TDI/n-PrOH/ϵ-caprolactam is AC.

3.3. Discussion of Kinetics Data. It is well know that in aromatic diisocyanates, where the isocyanate groups are located at the same aromatic ring, substituent effects cannot be neglected and that the kinetic scheme for the reaction of a monoalcohol with TDI is based on two parallel and two subsequent reactions (see Scheme 6). Each reaction step is usually considered to follow a second-order kinetics depending on the concentration of isocyanate and alcohol, thus resulting in a quite complicated mathematical description.[10,21] The

Scheme 6

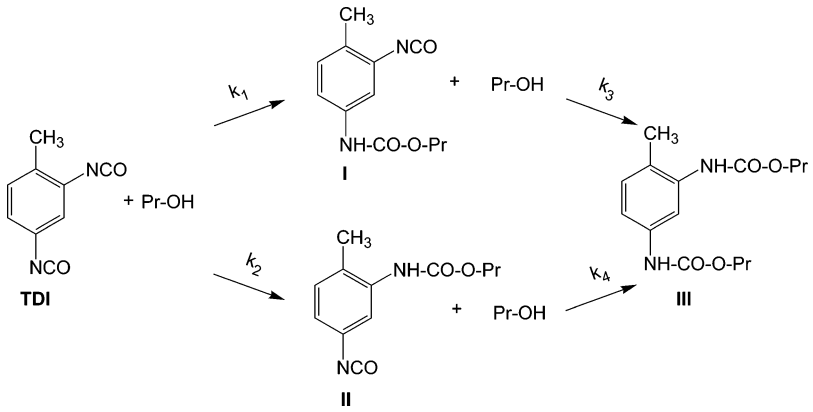

rate of change in the concentration of all the involved species obeys the following set of kinetic equations:

$$\frac{d[TDI]}{dt} = -k_1[TDI][nPrOH] - k_2[TDI][nPrOH] \quad (1)$$

$$\frac{d[I]}{dt} = k_1[TDI][nPrOH] - k_3[I][nPrOH] \quad (2)$$

$$\frac{d[II]}{dt} = k_2[TDI][nPrOH] - k_4[II][nPrOH] \quad (3)$$

$$\frac{d[III]}{dt} = k_3[I][nPrOH] + k_4[II][nPrOH] \quad (4)$$

$$\frac{d[nPrOH]}{dt} = -k_1[TDI][nPrOH] - k_2[TDI][nPrOH] - k_3[I][nPrOH] - k_4[II][nPrOH] \quad (5)$$

where I and II are the addition products of one molecule of alcohol to the isocyanate in position *para* and *ortho* to the methyl group on the aromatic moiety, respectively (see Scheme 6). III is the addition product of two alcohol molecules to TDI.

By solving such equations with the following assumptions

$$\frac{k_3}{k_1 + k_2} \ll 1 \quad \text{and} \quad \frac{k_4}{k_1 + k_2} \ll 1 \quad (6)$$

the variation in time of the concentration of two isocyanate groups is described by the following equation:

$$\frac{[NCO]}{[NCO]_0} = \frac{2[TDI] + [I] + [II]}{2[TDI]_0} = \frac{C_2 + C_3}{\{C_1[TDI]_0 + C_2 + C_3\}e^{(C_2+C_3)(k_1+k_2)t} - C_1[TDI]_0} \times \left[1 - \frac{1}{2}\left(\frac{k_1}{k_1 + k_2 - k_3} + \frac{k_2}{k_1 + k_2 - k_4}\right)\right] + \frac{1}{2}\frac{k_1}{k_1 + k_2 - k_3} \times \left(\frac{C_2 + C_3}{\{C_1[TDI]_0 + C_2 + C_3\}e^{(C_2+C_3)(k_1+k_2)t} - C_1[TDI]_0}\right)^{k_3/(k_1+k_2)} + \frac{1}{2}\frac{k_2}{k_1 + k_2 - k_4} \times \left(\frac{C_2 + C_3}{\{C_1[TDI]_0 + C_2 + C_3\}e^{(C_2+C_3)(k_1+k_2)t} - C_1[TDI]_0}\right)^{k_4/(k_1+k_2)} \quad (7)$$

By applying a fitting procedure to the experimental data by using eq 7, the kinetic constants reported in Table 1 are obtained. Despite the model capacity to describe the experimental concentration decrease in time, this model is rejected because of the failure of the assumptions reported in (6). In fact, the values of the constants obtained through the fitting procedure with eq 7 yield

$$\frac{k_3}{k_1 + k_2} \ll 1 \quad \text{and} \quad \frac{k_4}{k_1 + k_2} \cong 1 \quad (8)$$

By solving eqs 1−5 with eq 8, the variation in time of the concentration of isocyanate groups is

$$\frac{[NCO]}{[NCO]_0} = \frac{C_2}{\{(C_1 + C_3)[TDI]_0 + C_2\}e^{C_2(k_1+k_2)t} - (C_1 + C_3)[TDI]_0} \times \left[1 - \frac{1}{2}\left(\frac{k_1}{k_1 + k_2 - k_3} + \frac{k_2}{k_1 + k_2 - k_4}\right)\right] + \frac{1}{2}\frac{k_1}{k_1 + k_2 - k_3} \times \left(\frac{C_2}{\{(C_1 + C_3)[TDI]_0 + C_2\}e^{C_2(k_1+k_2)t} - (C_1 + C_3)[TDI]_0}\right)^{k_3/(k_1+k_2)} + \frac{1}{2}\frac{k_2}{k_1 + k_2 - k_4} \times \left(\frac{C_2}{\{(C_1 + C_3)[TDI]_0 + C_2\}e^{C_2(k_1+k_2)t} - (C_1 + C_3)[TDI]_0}\right)^{k_4/(k_1+k_2)} \quad (9)$$

Details on derivation of eqs 7 and 9 are given as Supporting Information.

By applying a fitting procedure to the experimental data by using eq 9, the kinetic constants reported in Table 1 are obtained. The assumption in (6) is found to be true for reactions 1 and 3, whereas it is not exactly verified for reactions 2 and 4, where the $k_4/(k_1 + k_2)$ ratio is 0.56 and 0.66, respectively. In addition, the reported values of the kinetic constants for reactions 1 and 3 should also be considered as approximated data, even if they are affected by lower errors with respect to reactions 2 and 4. In fact, both the experimental and theoretical approaches here used are not completely rigorous: as a result, the estimated values are useful for comparison purposes between reactions carried out under similar experimental conditions. However, the low values of the χ^2 parameter resulting from the fitting procedure indicate the capability of the model to describe the experimental data. In particular, the best

Table 1. Kinetic Constants and χ^2 for the Fitting of Experimental Data[a]

	I TDI + n-PrOH	**II** TDI + n-PrOH + ϵ-caprolactam	**III** TDI + n-PrOH + AC	**IV** TDI+ ϵ-caprolactam
		First Approximation (Eq 7)		
$\chi^2 \times 10^5$	10	3	5	13
$k_1 \times 10^3$ [mol^{-1} min^{-1} L]	0.1959 ± 0.0020	71.0 ± 2.7	2.083 ± 0.055	359 ± 40
$k_2 \times 10^3$ [mol^{-1} min^{-1} L]	0.0788 ± 0.0071	41.4 ± 2.8	0.773 ± 0.035	353 ± 50
$k_3 \times 10^3$ [mol^{-1} min^{-1} L]	0.00836 ± 0.00058	2.74 ± 0.13	0.1042 ± 0.0034	16.7 ± 1.8
$k_4 \times 10^3$ [mol^{-1} min^{-1} L]	2.6105 ± 0.0050	35.64 ± 0.37	2.428 ± 0.060	261 ± 14
		Second Approximation (Eq 9)		
$\chi^2 \times 10^5$	1	2	2	16
$k_1 \times 10^3$ [mol^{-1} min^{-1} L]	104.9 ± 6.6	186.6 ± 2.0	155.4 ± 8.3	1756 ± 56
$k_2 \times 10^3$ [mol^{-1} min^{-1} L]	34.8 ± 1.7	98.0 ± 1.9	53.0 ± 2.1	1533 ± 72
$k_3 \times 10^3$ [mol^{-1} min^{-1} L]	0.712 ± 0.043	9.729 ± 0.067	7.225 ± 0.069	116.2 ± 3.8
$k_4 \times 10^3$ [mol^{-1} min^{-1} L]	170 ± 11	159.5 ± 7.7	233 ± 15	2170 ± 170

[a] The k_i (i = 1, 2, 3, 4) are kept as adjustable parameters.

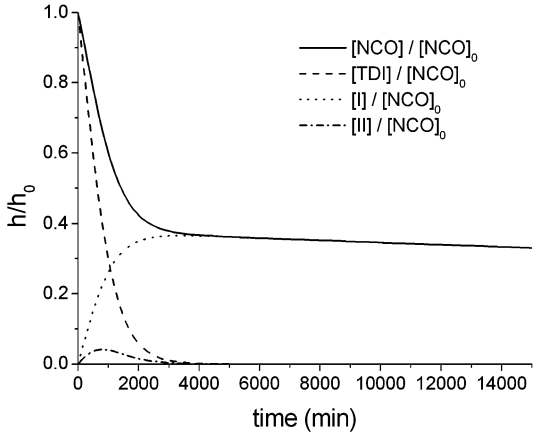

Figure 5. Plots obtained from the semiempirical model depicting the total reaction proceeding in time for the reaction between TDI and n-PrOH (1) carried out in CCl_4 at room temperature.

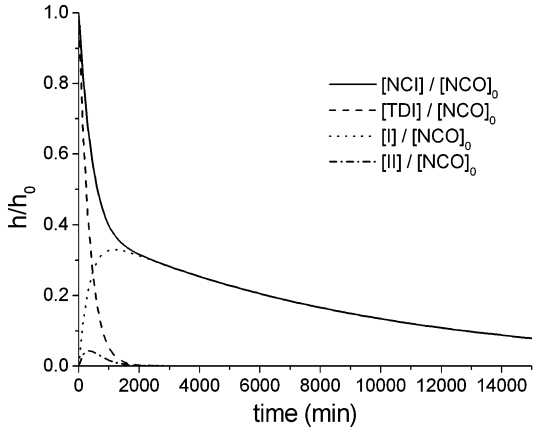

Figure 6. Plots obtained from the semiempirical model depicting the total reaction proceeding in time for the reaction between TDI and n-PrOH (1) carried out in CCl_4 at room temperature in the presence of a catalytic amount of AC.

fitted case ($\chi^2 = 9.86 \times 10^{-6}$) is the reference reaction 1 (TDI/n-PrOH) whereas reaction 4 (TDI + ϵ-caprolactam) is the worst ($\chi^2 = 1.6 \times 10^{-4}$). This is not surprising. In fact, the kinetics of the elementary steps for reaction **I** has been widely investigated in the literature and is reported to follow a second-order kinetics. (On the contrary, to the best of our knowledge no detailed investigations have been performed on the kinetics of the reaction of addition of ϵ-caprolactam to TDI.) Furthermore, deviations from the model can also be caused by secondary reactions such as dimerization and trimerization of the isocyanate, alcohol self-association effects, association of alcohol with the forming urethane,[6,11,22] and reactions with humidity, which are all neglected by the model.

The values of the calculated constants for the first addition steps (k_1 and k_2) are in accordance with the value reported by Cotarga et al.[11] for the reaction between TDI and monohydroxylic alcohols in carbon tetrachloride at 32 °C.

The kinetic constants seem to indicate that the observed reaction rate is initially governed by the rate of consumption of TDI whereas for longer times it is governed by the rate of consumption of I. In Figure 5 the rates of each individual reaction step as obtained from the semiempirical model are shown. The amount of II formed during the reaction time is quite negligible because the rate of formation of II is smaller than the rate of formation of I. In addition, II does not accumulate because its consumption rate is higher than its formation rate. The k_3 constant is taken into account for the slowing down of the reaction. At this stage the reaction rate becomes comparable to that of TDI with water, which is in competition with the former.

The addition of a catalytic amount of ϵ-caprolactam to the TDI/n-PrOH mixture increases the rate of all reaction steps even if the mostly affected (besides the addition of n-PrOH to I) is the slowest step, as results from the comparison of the relative kinetic constants of the elementary steps. Moreover, k_1 and k_2 may be overcount in reaction 2 because of the parallel reaction of ϵ-caprolactam with TDI at the first stage of the process. The difference in the reactivity between n-PrOH and ϵ-caprolactam is evidenced by the larger discrepancies in the kinetic constants for the addition of ϵ-caprolactam (reaction 4) than n-PrOH (reaction 1). The presence of the parallel reaction of TDI with alcohol and ϵ-caprolactam at the initial reaction stage for the reaction catalyzed by ϵ-caprolactam (reaction 2) also accounts for the differences observed between the reactions catalyzed by ϵ-caprolactam (2) and AC (2). The comparison of the constants for the reaction catalyzed by AC (3) and the uncatalyzed reaction 1 confirms the accelerating effect of AC in the urethane formation reaction, and in particular it is evident that the catalyst mostly affects the slowest process (k_3), which determines the reaction rate at larger reaction times. This is clearly evidenced by Figure 6, where the simulation of the kinetics of each elementary step of the addition reaction is shown. By comparing the graphics with what was reported in Figure 5 for the uncatalyzed reaction 1, it is evident that both the reactions of formation and consumption of I are accelerated by AC.

Table 2. Kinetic Constants and Correlation Coefficients for the Fitting of Experimental Data with Eq 9[a]

AC [mol × 10^6]	$CHCl_3$ [μL]	$\chi^2 \times 10^5$	$k_1{}^b \times 10^3$ [mol^{-1} min^{-1} L]	$k_2{}^b \times 10^3$ [mol^{-1} min^{-1} L]	$k_3{}^b \times 10^3$ [mol^{-1} min^{-1} L]	$k_4{}^b \times 10^3$ [mol^{-1} min^{-1} L]
0	0	1	104.9 ± 6.6	34.8 ± 1.7	0.712 ± 0.043	170 ± 11
0.151	12	3	219.3 ± 4.5	100.0 ± 2.2	6.29 ± 0.08	281 ± 11
0.163	13	9	216.8 ± 8.0	81.9 ± 3.1	3.96 ± 0.08	269 ± 20
0.172	5	2	155.4 ± 8.3	53.0 ± 2.1	7.225 ± 0.069	233 ± 15
0.176	14	23	381 ± 12	480 ± 38	9.7 ± 1.1	203 ± 10
0.225	13	5	856 ± 55	159.6 ± 8.4	42.96 ± 0.67	1300 ± 110
0.226	70	7	594 ± 34	146.1 ± 6.8	23.11 ± 0.38	817 ± 75
0.295	17	5	938 ± 49	191.5 ± 7.8	32.11 ± 0.38	1401 ± 98
0.589	34	13	575 ± 31	170.4 ± 9.7	20.73 ± 0.55	646 ± 93
0.880	70	5	469.2 ± 9.5	190.7 ± 7.8	16.19 ± 0.29	459 ± 33

[a] The k_i (i = 1, 2, 3, 4) are kept as adjustable parameters. [b] The standard deviation of each of the k_i which is obtained by the fitting is assumed as error.

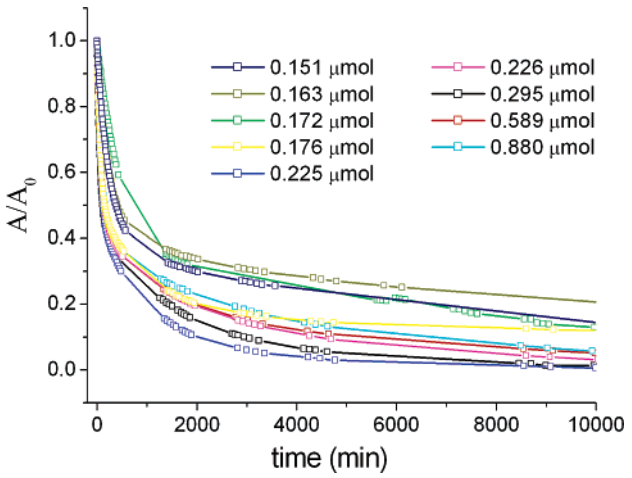

Figure 7. Comparison between the experimental decrease in time of the relative maximum absorbance of the IR stretching band of isocyanate in the range 2200−2300 cm^{-1} for the reaction between TDI and n-ProH (0.0166/0.0332 M in CCl_4) carried out in the presence of the catalytic amounts of AC listed in the legend.

3.4. Effect of AC Concentration. To better analyze the catalytic activity of ϵ-caprolactam in the reaction of formation of urethane linkages, different TDI/n-PrOH/AC/chloroform mixtures with different amounts of AC were prepared (see Table 2 for the quantities of AC added to 2 mL of CCl_4 diisocyanate/alcohol solutions 1:1 in volume). Chloroform was used to dissolve AC: see again Table 2 for solvent amounts used in each test.

The rate of decrease of the isocyanate IR stretching band shows an irregular dependence on the catalyst concentration, as is shown in Figure 7. This behavior can be partially clarified by analyzing each kinetic curve with the aid of the model given in eq 9, which provides the kinetic constants reported in Table 2. All χ^2 values are lower than 0.00023, thus indicating a good correspondence between the model and the experimental data for all cases. The estimated values for k_1 and k_2 show an increasing dependence on the catalyst concentration and, on the contrary, a decreasing dependence on the chloroform amount. This is clearly evidenced by the data reported in the 3D graphics of Figure 8. A possible reason for such behavior can be competition between AC and chloroform with respect to reactants, for example, as a result of hydrogen-bonding interactions.

A rough analysis of the dependence of the observed kinetic constants on the AC amount by excluding the chloroform inhibition effect seems to indicate that the rate of reaction between TDI and n-PrOH increases as

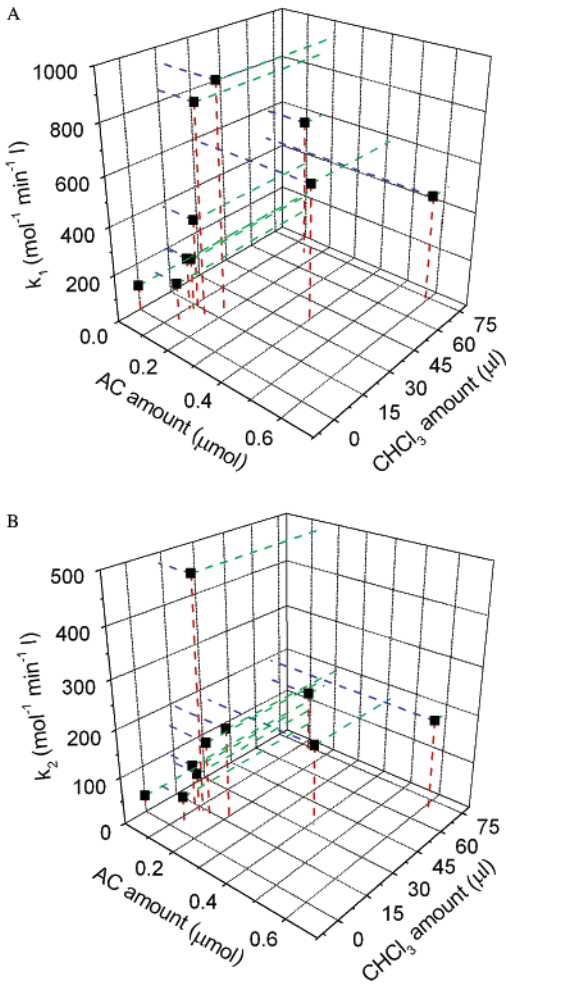

Figure 8. 3D plots for the observed second-order kinetic constants (plot A for k_1 and plot B for k_2) for the reaction between TDI and n-PrOH (1) carried out in CCl_4 at room temperature in the presence of different catalytic amounts of AC. On the y axis the chloroform amounts used to dissolve each AC amount are reported.

the catalyst amount increases until the ratio between AC and n-PrOH of 0.06 is reached. For higher ratios no further accelerating effects seem to occur; on the contrary, a decreasing catalytic activity is observed. This behavior may be due to the limited solubility of AC in the solvent mixture and to the already mentioned inhibiting effects of chloroform.

3.5. Quantum Mechanical Calculations. To try to identify the chemical features of AC which are responsible for its catalytic activity, the determination of the chemical structure of the molecule would be necessary.

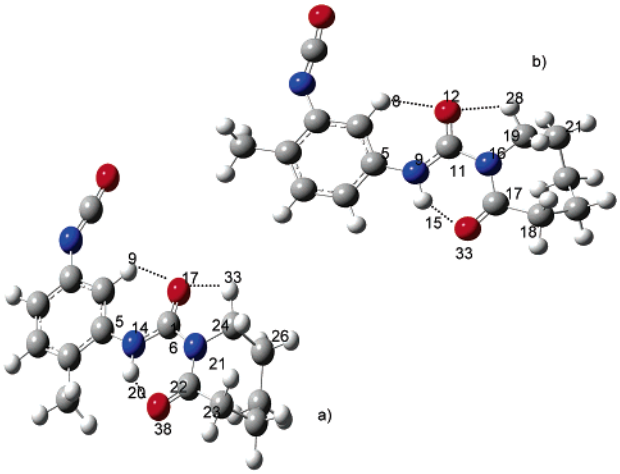

Figure 9. Calculated structures of AC monoadducts: (a) reaction of the isocyanate groups in ortho with respect to the methyl group and (b) reaction of the isocyanate groups in para with respect to the methyl group.

Table 3. Geometrical Parameters (Distances and Angles) for the AC Adduct Obtained from the Reaction of the Isocyanate Groups in *Ortho* with Respect to the Methyl Group (See Text for Details)

	R (Å)		angle (deg)
C5−N14	1.413	C5−N14−C16	127.7
N14−H20	1.022	N14−C16−N21	115.6
N14−C16	1.362	C16−O17−H9	103.7
C16−O17	1.225	C16−O17−H33	87.9
O17−H9	2.155	C16−N21−C22	125.8
O17−H33	2.172	C16−N21−C24	115.0
C16−N21	1.446	N21−C22−O38	123.1
N21−C22	1.390	C22−O38−H20	102.2
N21−C24	1.481	N14−C16−N21−C24	−180.0
C22−O38	1.235	C16−N21−C24−C26	−101
O38−H20	1.769	C16−N21−C22−C23	177.0

Table 4. Geometrical Parameters (Distances and Angles) for the AC Adduct Obtained from the Reaction of the Isocyanate Groups in *Para* with Respect to the Methyl Group (See Text for Details)

	R (Å)		angle (deg)
C5−N9	1.409	C5−N9−C11	127.4
N9−H15	1.022	N9−C11−N16	115.1
N9−C11	1.360	C11−O12−H8	103.8
C11−O12	1.224	C11−O12−H28	87.6
O12−H8	2.195	C11−N16−C17	125.7
O12−H28	2.169	C11−N16−C19	114.8
C11−N16	1.446	N16−C17−O33	123.4
N16−C17	1.391	C17−O33−H15	102.1
N16−C19	1.478	N9−C11−N16−C19	180.0
C17−O33	1.232	C11−N16−C19−C21	−100.0
O33−H15	1.764	C11−N16−C17−C18	176.6

However, it was not possible to obtain AC crystals suitable for a structure determination by conventional X-ray analysis; for this reason, to obtain a prediction of the molecular structure of AC and to clarify its structural features leading the catalytic activity, a B3LYP/6-31+G* quantum mechanical study on AC has been performed. In particular, because of the quite large number of degrees of freedom of the molecule, the calculations were limited to the structure of the complex obtained by the reaction of TDI with only one molecule of ϵ-caprolactam. Stable structures are predicted in the case of both the ortho and para reaction (see Figure 9 and Tables 3 and 4 and for pictures and selected geometrical parameters). The deviation in the geometrical parameters of the urethane-like portion between the two isomers is less that 0.3% on average and never larger than 1.9% for the single parameter. This indicates a substantial equivalence in structure of the two isomers. In both cases, the analysis of the oxygen−hydrogen distances evidences the possible presence in the structures of three intramolecular hydrogen bonds, which are indicate by dotted lines in Figure 9.

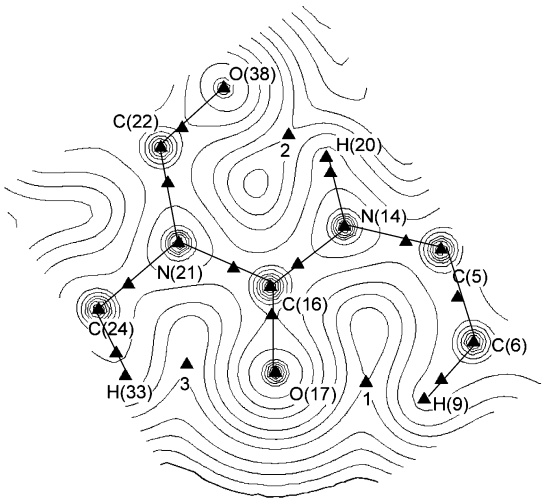

Figure 10. AIM map of the electron density of a selected portion of AC.

Because of the substantial equivalence in the two isomers, in the following we will focus on the ortho isomer only. To consider the change in geometry arising from effects due to a solvent environment, geometry optimizations were repeated in CCl_4, $CHCl_3$, and n-PrOH. The average deviation between the geometrical parameters calculated in a vacuum and in solution is 0.16% in CCl_4, 0.18% in $CHCl_3$, and 0.34% in n-PrOH, thus indicating that the urethane-like structure is quite rigid and only little affected by environmental effects. It should be noticed, however, that our solvation model is purely electrostatic and does not explicitly take into account specific solute−solvent interactions (for example, hydrogen bonding). Nonetheless, in the following, based on the slight difference arising from the presence of the solvation environment, the discussion will be limited to the structure calculated for the isolated system.

To characterize the calculated structure and to evidence the presence of hydrogen bonding from the electronic point of view, in Figure 10 the map of the electronic density as calculated by exploiting the Bader's atoms in molecules analysis is reported. We recall that the AIM analysis is based on a topological characterization of the electron density distribution and considers the presence of a (3, −1) bond critical point between two atoms (indicated by a triangle in Figure 10) as a necessary and sufficient condition for the presence of a chemical bond.[18c] Besides the presence in the structure of AC of such critical points related to covalent bonds, the analysis of the electron density distribution in AC reveals the presence of three additional (3,−1) bond critical points between H(9) and O(17), H(20) and O(38), and H(33) and O(17), labeled 1, 2, and 3, respectively, in Figure 10. These critical points are related to the presence of three intramolecular hydrogen bonds. It has been reported that the value of the electron density ρ and its Laplacian $\nabla^2\rho$ at the bond critical points (3, −1) correlate with the bond energy.[18] The values of such indexes for selected bonds of AC are reported in Table 5. The charge densities at bond critical points of the

Table 5. Electron Density, Its Laplacian $\nabla^2\rho$, and Ellipticity ϵ at Selected Bond Critical Points of AC

	$10^2\rho$	$10^2\nabla^2\rho$	$10^2\epsilon$
N(14)−H(20)	32.116	−40.3806	
C(6)−H(9)	28.272	−25.9443	
C(24)−H(33)	28.404	−25.8269	
1 O(17)−H(9)	2.0000	1.80904	10.6612
2 O(38)−H(20)	4.2088	3.59749	1.02342
3 O(17)−H(33)	2.1964	2.29359	88.8425

Table 6. Natural Atomic Charges of Selected Atoms of (*Ortho*) AC and ϵ-Caprolactam (Atomic Units)

atom	charge	atom	charge
AC: H(9)	0.27975	AC: H(benzenic, medium)	0.24750
AC: O(17)	−0.64571	ϵ-caprolactam: H (medium)	0.24608
AC: H(20)	0.46232	ϵ-caprolactam: H (amidic)	0.43207
AC: H(33)	0.29159	ϵ-caprolactam: O	−0.64127
AC: O(38)	−0.63486		

Table 7. Natural Atomic Charges of Selected Atoms of AC, ϵ-Caprolactam, and DABCO (Atomic Units)

atom	charge
AC: N(14)	−0.64552
AC: N(21)	−0.52685
ϵ-caprolactam: N	−0.68098
DABCO: N	−0.52225

hydrogen bonds (1, 2, and 3) are an order of magnitude smaller than that found for a covalent bond (compare values in Table 5) and all within the ranges reported in the literature (see, for example, ref 23). In addition, the values of the Laplacian of the charge density at bond critical points 1, 2, and 3 are positive: this is a further necessary condition to define hydrogen bonding. Also, the range of values here obtained compare very well with the range reported in the literature for hydrogen bondings, 0.024−0.139 au.[23a] In summary, from the AIM analysis, the presence of three hydrogen bonds in AC can be stated. In more detail, we note that the strength of the H bond involving O(38) and H(20) is double the value of the O(17)−H(9) and O(17)−H(33) H bonds. Moreover, the ellipticity values reported in Table 5 show a larger instability of the O(17)−H(9) and O(17)−H(33) H bonds with respect to the O(38)−H(20) bond: in addition, among the three H bonds, O(17)−H(33) is the least stable. All these findings are not unexpected and correlate well with the bond distances, being 1.769 Å for O(38)−H(20), 2.155 Å for O(17)−H(9), and 2.172 Å for O(17)−H(33).

To further characterize hydrogen bonding in AC, in Table 6, natural atomic charges of selected atoms of AC are reported: for comparison, natural atomic charges of selected atoms of ϵ-caprolactam are also shown. Notice that natural charges of either H(20) or H(33) and H(9) are more positive than the corresponding ones of similar atoms not involved in hydrogen bonding.

To further characterize AC, in Table 7 the natural charges of selected atoms of it are shown in comparison with charges of relevant atoms of ϵ-caprolactam and 1,4-diazabicyclo[2.2.2]octane (DABCO), which is commonly used as catalyst in the polyurethane formation reaction.[5] We note that N(21) in AC has a charge very similar to the corresponding atom in DABCO. (The charge of N(14) is instead more similar to that of the nitrogen atom in ϵ-caprolactam, but less negative.) These findings can suggest that, as a result of the formation of AC, the formation of a DABCO-like catalytic center occurs. Perhaps, the catalytic effect is lead by the lone-pair like orbital of N atomic centers. In particular, it is possible

Scheme 7

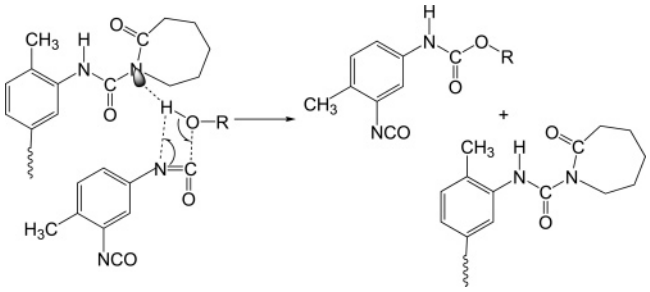

that the N(21) lone-pair-like orbital, which essentially has a *p* character, coordinates the acidic H of n-PrOH, thus favoring the further attack of the alcoholic oxygen atom to the carbonylic center, which will result in the formation of the urethane and which will form back the precursor catalyst (ϵ-caprolactam) (see Scheme 7).

Such an hypothesis is also in accordance with the findings that were shown in the previous section, i.e., the inhibiting effect of chloroform on the reaction kinetics. In fact, coordination between the acidic H atom of chloroform and the N(21) center of AC can occur, thus resulting in competition between n-PrOH and chloroform for the catalytic site.

4. Summary and Conclusions

The experimental work here reported and the analysis of the kinetic parameters obtained through the kinetic model given by eq 9 have shown the accelerating role of ϵ-caprolactam in the reaction of formation of urethane linkages from isocyanates and alcohol. In particular, it has been demonstrated that ϵ-caprolactam is the precursor of the active catalytic species, which in the case in study is the acylurea-like derivative AC: 1-methyl-2,4-[(2-oxoazepane-1-carbonyl)amino]benzene, which is formed in situ as a result of the reaction between TDI and ϵ-caprolactam.

The catalyzed reaction follows a second-order kinetics with respect to the reactants; however, a not completely clarified dependence on the amount of catalyst is found. This should indicate that TDI or n-propanol participate with AC to the formation of the activated complex of the rate-determining step of the reaction. However, on the basis of the experimental data reported, it is not possible to assess which one, between TDI and n-propanol, is the activated species. In addition, to the best of our knowledge, no additional data are available in the literature to help us in the explanation of the origin of the catalytic activity of AC. To further investigate this point, and due to the impossibility of obtaining AC crystals suitable for X-ray analysis, the molecular structure of AC has been predicted by quantum mechanical calculations. Such calculations have in some way clarified AC structural features leading the catalytic activity, showing, in particular, the formation of a DABCO-like catalytic center. A possible catalysis mechanism has been proposed, involving the N(21) lone-pair-like orbital coordinating the acidic H of n-PrOH, thus favoring the attack of the alcoholic oxygen atom to the carbonylic group.

Acknowledgment. The authors thank Prof. Francesco Ciardelli for useful discussion and revising the manuscript. The authors are also indebt to Prof. Mauro Isola for useful discussions and suggestions on the kinetic model. The authors also thank Dr. Leonardo

Andreotti (Gruppo X, Marghera) for useful discussions and suggestions. Partial support by Alcan Packaging (Lugo di Vicenza, Italy) and MIUR (Ministero dell' Istruzione, Università e Ricerca) is here acknowledged.

Supporting Information Available: Derivation of the kinetic equations. This material is available free of charge via the Internet at http://pubs.acs.org.

References and Notes

(1) Ulrich, H. *Chemistry and Technology of Isocyanates*; Wiley: New York, 1996.
(2) Oertel, G. *Polyurethane Handbook*, 2nd ed.; Hanser Publishers: Munich, 1994.
(3) (a) Weber, K. A.; Wagner, K.; Klipfel, S. (Bayer, A.-G.; Fed. Rep. Ger.). Ger. Offen. 1975, DE2330175. (b) Rasmussen, M. O. H.; Rasmussen, J.; Rasmussen, P. M. (Curex APS, DK), DAN. **1997**, DK171704, DK9500846. (c) Siegfried, H.; Schneidinger, F.; Schetschok, H. G. (Morton International GmH, Germany) Ger. Offen. 1994, DE4229953.
(4) Wicks, D. A.; Wicks, Z. W., Jr. *Prog. Org. Coat.* **1999**, *36*, 148.
(5) Satchel, D. P. N.; Satchel, R. S. *Chem. Soc. Rev.* **1975**, *4*, 231.
(6) Thiele, L.; Becker, R. *Adv. Urethanes Sci. Technol.* **1995**, *12*, 59.
(7) Caraculacu, A. A.; Coseri, S. *Prog. Polym. Sci.* **2001**, *26*, 799.
(8) (a) Farkas, A.; Mills, G. A. *Adv. Catal.* **1962**, *13*, 393. (b) Entelis, S. G.; Nesterov, O. V. *Russ. Chem. Rev.* **1966**, *35*, 917. (c) Petrus, A. *Int. Chem. Eng.* **1971**, *11*, 314. (d) Sarynina, L. I.; Evreinov, V. V.; Khodzhasva, E. K.; Entelis, S. G. *Kinet. Catal.* **1972**, *13*, 314. (e) Raspoet, G.; Nguyen, M. T.; McGarraghy, M.; Hegarty, A. F. *J. Org. Chem.* **1998**, *63*, 6878.
(9) Baker, J. W.; Holdsworth, J. B. *J. Chem. Soc.* **1947**, 713.
(10) (a) Hetfleys, J.; Svoboda, P.; Jakcubkova, M.; Chvalovsky, V. *Collect. Czech. Chem. Commun.* **1973**, *38*, 717. (b) Farkas, A.; Strohm, P. F. *Ind. Eng. Chem. Fundam.* **1965**, *4*, 32. (c) Farkas, A.; Flynn, K. G. *J. Am. Chem. Soc.* **1960**, *82*, 642. (d) Burkus, J. *J. Org. Chem.* **1962**, *27*, 474. (e) Dyer, E.; Gelnn, J. F.; Lendrat, E. G. *J. Org. Chem.* **1961**, *26*, 2919.
(11) Bacaloglu, R.; Cotarga, L.; Marcu, N.; Tolgyi, S. *J. Prakt. Chem.* **1988**, *330*, *4*, 530.
(12) Chang, M. C.; Chen, S. A. *J. Polym. Sci., Polym. Chem. Ed.* **1987**, *25*, 2543.
(13) Koch, W.; Holthausen, M. A. *A Chemist's Guide to Density Functional Theory*; Wiley-VCH: Berlin, 2001.
(14) Frisch, M. J.; Trucks, G. W.; Schlegel, H. B.; Scuseria, G. E.; Robb, M. A.; Cheeseman, J. R.; Montgomery, J. A. Jr.; Vreven, T.; Kudin, K. N.; Burant, J. C.; Millam, J. M.; Iyengar, S. S.; Tomasi, J.; Barone, V.; Mennucci, B.; Cossi, M.; Scalmani, G.; Rega, N.; Petersson, G. A.; Nakatsuji, H.; Hada, M.; Ehara, M.; Toyota, K.; Fukuda, R.; Hasegawa, J.; Ishida, M.; Nakajima, T.; Honda, Y.; Kitao, O.; Nakai, H.; Klene, M.; Li, X.; Knox, J. E.; Hratchian, H. P.; Cross, J. B.; Adamo, C.; Jaramillo, J.; Gomperts, R.; Stratmann, R. E.; Yazyev, O.; Austin, A. J.; Cammi, R.; Pomelli, C.; Ochterski, J. W.; Ayala, P. Y.; Morokuma, K.; Voth, G. A.; Salvador, P.; Dannenberg, J. J.; Zakrzewski, V. G.; Dapprich, S.; Daniels, A. D.; Strain, M. C.; Farkas, O.; Malick, D. K.; Rabuck, A. D.; Raghavachari, K.; Foresman, J. B.; Ortiz, J. V.; Cui, Q.; Baboul, A. G.; Clifford, S.; Cioslowski, J.; Stefanov, B. B.; Liu, G.; Liashenko, A.; Piskorz, P.; Komaromi, I.; Martin, R. L.; Fox, D. J.; Keith, T.; Al-Laham, M. A.; Peng, C. Y.; Nanayakkara, A.; Challacombe, M.; Gill, P. M. W.; Johnson, B.; Chen, W.; Wong, M. W.; Gonzalez, C.; Pople, J. A. *Gaussian03,* Revision A.1; Gaussian, Inc.: Pittsburgh, PA, 2003.
(15) (a) Becke, A. D. *Phys. Rev. A: At., Mol., Opt. Phys.* **1988**, *38*, 3098. (b) Becke, A. D. *J. Chem. Phys.* **1993**, *98*, 5648.
(16) Hehre, W. J.; Radom, L.; Schleyer, P. V.; Pople, J. A. *Ab initio Molecular Orbital Theory;* Wiley: New York, 1986.
(17) (a) Reed, A. E.; Weinhold, F. J. *Chem. Phys.* **1983**, *78*, 4066. (b) Reed, A. E.; Weinstock, R. B.; Weinhold, F. *J. Chem. Phys.* **1985**, *83*, 735. (c) Weinhold, F. In *Encyclopedia of Computational Chemistry*; Schleyer, P. v. R., Allinger, N. L., Clark, T., Gasteiger, J., Kollman, P. A., Schaefer, H. F. III, Schreiner, P. R., Eds.; Wiley: Chichester, UK, 1998; Vol. 3, p 1792.
(18) (a) Bader, R. F. W. *Atoms in Molecules: A Quantum Theory*; Oxford University Press: Oxford, 1994. (b) Bader, R. F. W. *Chem. Rev.* **1991**, *91,* 893. (c) Bader, R. F. W. *J. Phys. Chem. A* **1998**, *102,* 7314.
(19) (a) Biegler-König, F.; Schönbohm, J.; Bayles, D. *J. Comput. Chem.* **2001**, *22*, 545. (b) Biegler-König, F.; Schönbohm, J. *J. Comput. Chem.* **2002**, *23*, 1489.
(20) (a) Tomasi, J.; Persico, M. *Chem. Rev.* **1994**, *94*, 2027. (b) Tomasi, J.; Cammi, R.; Mennucci, B.; Cappelli, C.; Corni, S. *Phys. Chem. Chem. Phys.* **2002**, *4*, 5697.
(21) Agherghinei, I.; Prisacariu, Cr.; Caraculacu, A. A. *Rev. Roumaine Chim.* **1991**, *36*, 1135.
(22) Schwetlick, K.; Noack, R. *J. Chem. Soc., Perkin. Trans.* **1995**, *2*, 395.
(23) (a) Koch, U.; Popelier, P. L. A. *J. Phys. Chem.* **1995**, *99*, 9747. (b) Popelier, P. L. A.; Logothetis, G. *J. Organomet. Chem.* **1998**, *555*, 101.

MA0480998